Proceedings of Engineering & Technology (PET)
pp. 127-133

SIFT/LBP 3D face recognition

Narimen SAAD[1] NourEddine DJEDI
Department of Computer Science
LESIA Laboratory
University of Biskra, Algeria
[1]saad_narimen@live.fr

***Abstract*— 3D face recognition is a promising alternative to face the problem of recognizing 2D robustness. Therefore, the main advantage of 3D face recognition-based approach uses all the information on the geometry of the face, which allows us to get an accurate representation of the face. In the proposing contribution all distinctive facial features are captured by first extracting SIFT (Scale Invariant Feature Transform) key points, then we applied the operator SIFT on $LBP_{P,R}$ (Local Binary Pattern) images, separately. Following the work of Faltemier and al. [7] then Tang and al. [22] we can better detect a number of key points by using SIFT on $LBP_{P,R}$ images, that using SIFT on the original images of the face analysis then measuring how the face changes along profiles, built between pairs of key points.**

The contribution is tested using whole of the Face Recognition Grand Challenge FRGC v1.0 data. Finally, we perform a classification based on SVM process.

Keywords—3D biometric model, Biometrics, Face recognition.

I. INTRODUCTION

In recent years, approaches of recognition faces in 2D still working with images and videos have gated a very great precision that can even surpass face recognition of human capabilities.

Though, face recognition is ever a hard task, particularly computer vision if the lighting conditions or pose issues are not verified. Not long ago, the accessibility of 3D facial data acquired with scanners has increased interest for 3D facial testing solutions using 3D facial form to improve recognition accuracy. In fact, it is expected the 3D geometry of the face to have less sensitivity to variations in illumination or pose changes. Since the last Face Recognition Grand Challenge (FRGC 2005) [14], a lot of 3D face recognition approaches have been proposed and tested (for further discussion, see the investigation in [4], and survey of the literature [2, 8, 11].

In summary, 3D face recognition approaches can be classed in two broad classes: global (or holistic) perform face matching from representations extracted from the total face; and the partition of the local region (or base-region), the face in the regions, and the extract and match suitable descriptors for each of them. There are also hybrid solutions that combine global and local descriptors and multimodal solutions incorporating 2D and 3D information to improve recognition accuracy [19].

In general, the overall results are obtained from the whole surface of the face, which usually makes the compact and therefore efficient calculation. Holistic representations are robust to noise, although they are sensitive to face alignment and missing parts, and the precision of recognition is gravely concerned if the 3D model of the face is obstructed by the hair, ears and neck. In inclusion, precision significantly decreases in the presence of non-neutral facial expressions.

Nevertheless, the local representatives are from small parcels on the surface of the face, which can even reduce to small regions throughout identified key points. The feature characterizing local approaches is their potential to deal with missing parts, facial expressions and occlusions: Of the description of the face results from the combination of local descriptors computed for many parts of the face, missing parts or deformation some parts due to blocked or non-neutral facial expression does not affect the combination together. After the high accounts, many recent approaches to 3D face recognition used local facial features much important ratios details on the reference databases such as the FRGC v 2.0 data [19].

In particular, certain new researches have exposed that the local descriptors based around salient key points can be usefully applied to represent 3D objects and faces. Within [12], a 3D-key point detection and descriptor inspired wide Invariant Feature Transform (SIFT) [9], was created and used to implement 3D face recognition using a hybrid 2D and 3D approach using also SIFT descriptor index detector 2D texture of face images [19].

Tang and al. [22] develop a 3D facial recognition algorithm using LBP (Local Binary Pattern) varieties of expression, operator extension LBP, which is widely used in the analysis of 2D face. First, to describe the human face more accurately and reduce the effect of its local distortion, a 3D facial division system is proposed. Then, for each region of the face, the statistical histogram is used to summarize the details of the face. Finally, 3D face recognition algorithm proposed is tested on BJUT-3D database and FRGCv2. The authors have obtained promising results and concluded that it is possible to apply the representation of LBP on 3D face recognition.

In this work, we propose a first contribution for 3D face recognition based on local properties of the face. The contribution is founded by the fact that the information captured by the SIFT descriptor in correlation to a selection of key points of the face is overly local to catch these traits characterizing the 3D face that support accurate facial recognition. Being enough discriminating these SIFT descriptors should be supplemented by data that model the morphological variations of the face among regions which are larger than the area used to extract SIFT descriptors. To do this, we introduce the profile face to model the depth of the long face analysis of a segment connecting two key points

ISSN: 2356-5608

SIFT. Specified a pattern of the face in the form of a range image, the SIFT model is used for the detection and description of key points. To describe features of the face that are captured by considering the SIFT descriptors of the detection key points and mesh the profile face that identified by each pair of key points. In comparing the two faces, SIFT descriptors are adapted to evaluate the resemblance between pairs of key points identified in the two range images. Then, the distance between both sides is obtained by calling the individual distances between the facial profiles which come from uniform key points. The suggested solution is proven using the dataset FRGC v1.0. To assess the accuracy of recognition in the existence of missing parts, we tacked an evaluation protocol where only the profiles that come from a part of the testing of the probe are estimated with gallery profiles scans. A second contribution 3D face recognition based on local properties of the face. The first contribution is improved by the fact that we use SIFT descriptor on LBP image for feature extraction 3D range images. For range images we use the LBP operator, the fusion of the four values of the radius LBP improves performance 2D and 3D information. [19]

The paper is organized as follows: In section 2, the important characteristics of the SIFT descriptor is summarized, and its adaptation to our contribution is detailed. The extraction of the face and profiles, defining the distance of similarity measure between the profiles using the SVM algorithm, a second contribution, that we use SIFT descriptor on LBP image for feature extraction 3D range images in section 5. The experiments with the proposed contribution and the results obtained on the FRGC v1.0 are reported. Finally, the discussion and conclusion are given in section 7.

II. SIFT KEY POINTS

The representation of the 3D model concerned face detection based on a number of key points on the 3D face surface and the description of the surface of the 3D face corresponding to the key points and along the paths linear linking pairs of key points. As opposed to possibilities that key points should correspond to face significant landmarks, such as eyebrows, eyes, mouth, cheeks, and nose, we perform particular supposition about the expected position of the-dots key on the facial surface.

Relatively, we include the position of key points to influence through specific morphological traits of each subject. In certain, supposing that the key point detection process incorporates a measure of the scale associated with every key point, we suppose that detected key points correspond to markers mean-full and operate the assumption so usually below the repeatability object: The most position | stable key points detected at coarse scales | do not change considerably in the models face the identical issue [19].

Consistent with this contribution, we used the SIFT algorithm to identify key points and description. SIFT were neither for 2D images in gray levels and cannot be immediately applied to the 3D face scans. Although, the 3D information of scanned face can be captured through the range of images that use the gray scale of each pixel to represent the depth of a facial scan.

These should be very particular, have nether offset probable be tolerant image noise and changes in lighting, and they must also be in the presence of practically invariant to range, rotation, unimportant changes in the management and visualization of local distortions. Although a lot of likely key points at different locations in an image can be detected, only the most distinctive and useful invariants for compatibility must be kept. These frequently fall on the edges and corners of the image, and can be of many different sizes and orientations as good. To detect key points, SIFT descriptors are calculated. In short, a SIFT descriptor for a little region of the image, e.g. 4x4 size is calculated from the vector gradient histograms of the pixels in the patch. Eight likely gradient directions, and therefore the total size of SIFT descriptor is 4x4x8 = 128 elements. This descriptor is unified to ameliorate invariance to changes in illumination (not relevant in the case of the range of images), and performed by other ways to ensure scale invariance and the rotation as well. These properties make the SIFT descriptor can issue a solid and powerful local representative of the range of the image and, consequently, of the face surface. In particular, SIFT descriptors were extracted using the following setting:

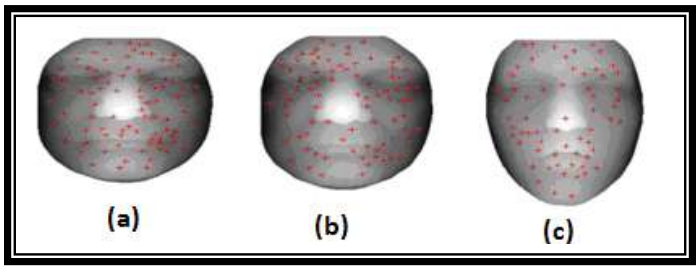

For example, Fig.1 shows the range of images from three 3D face scans;

- SIFT key points are extracted, and preserved their angles of range and orientation ;
- 4x4 Orientation histograms regions of each key point four sampling are used to calculate the SIFT descriptor [19].

As in Fig.1, detected by SIFT key points are presented for the range of images of three various analysis of the face. The prime two images represent the same subject, while the third is a different topic. In wide, the position of the key points on a detected face scanning depends on morphological features of the face. This is confirmed by the fact that the spatial arrangement of key points detected on different scans of the same subject | along a neutral expression | is much comparable. Though, the information that is captured by combining local descriptors (e.g. SIFT descriptors) with key points detected in a facial analysis is not sufficiently discriminating to support accurate recognition of the identity of the object. This is due to several reasons, which relate most significantly to the salience of local descriptors and inter-subject iterated. The latter refers to the absence of any warranty that the position of the key points on the face model should be separate on the subject. In fact, since the position of key points has a dependence on the morphology of the face, the detection of key points in models of different subjects understand a different layout on the face. Around the salience of local descriptors, calculated detected key points should be observed that these descriptors capture the morphology of the surface of the image in a small area

(typically 16x16 pixels) centered on the key point. The report that is retained is just enough to allow recognition of the part of the face that is the key point: the nose, one of the points' extreme mouth or eyes, etc. [19]

III. FACE PROFILES WITH SIFT key points

Two key points relating to SIFT detected on a range of picture to identify a face, its 1D function corresponding to the depth values corresponding along the points of the segment that connects the two key points. More formally, let:

- $\updownarrow(x)$ where $x \in \Re^2$ be the image of a range scanning of the face ;
- x_1, x_2 two key points ;

Then the profile identified by the ordered pair(x_1, x_2) is defined as:

- $\mathcal{P}_{I, x1,x2} = \updownarrow((1- t)\, x_1 + t x_2)$ $\quad t \in [0, 1]$ (1)

In describing the proposed model face, distinctive facial features are captured retaining SIFT key points descriptors detected on the range image and the profiles identified by pairs of these key points. The result data organized in a graph structure with nodes corresponding to the key points and edges corresponding to profiles.

SVM (Support Victor Machine) Technical supervised classification derived from the theory of statistical learning. The essential idea is to project data belonging to different classes not linearly separable, of the input space, in a larger space called feature space, so that the data becomes linearly separable [17].

In this space, the optimal hyper plane built in technique is used to compute the ranking function separating the classes.

Case of two classes:

$\{(x_1,y_1),\ldots.(x_n,y_n)\}$ where $y_i \in \{-1,+1\}$ and x_i input (2)

Given the graphics of the two faces, their dissimilarity is evaluated first assign to every node of the graph its first nearest node present in the second graph, proximity is measured as the Euclidean distance between the 128-dimensional SIFT descriptors related with the points- keys. Then, for each pair of corresponding nodes in the two graphs whole from profiles of the key points are compared to identify the two profiles with the minimum distance. Determined the generic profile P1 extract the pair of key points of the face analysis I1 and the profile P2 extract the pair (X3, X4) of key points of the face analysis I2 the distance between the two profiles is measured:

$$D(P1(t), P2(t)) = \int_0^1 |P1(t) - P2(t)|\, dt \quad (3)$$

Finally, the distance between the two faces of scans is measured by the average minimum distance values profiles on all pairs of correspondent nodes. Searching the linear classifier that separates the data with the lowest generation error. We result that, this classifier is a hyper-plane maximizes the margin of error, which is the sum of the distances between the hyper plane and the positive and negative models with the closest hyper plane [17]. In the case where the data cannot be divided by a linear function, the non linearity may be introduced by using a non-linear function. Consequently, the mapping plan can be used in the absence of modification reconciliation of just a partial playback side against a full analysis of the face. In this view, the suggested solution enables facial recognition even in the presence of parts and / or missing occlusions. The magnitude that the accessibility of only a part of a face affects the accuracy of the recognition is discussed in the next section.

IV. EXPERIMENTAL RESULTS (1)

In what follows, we present the results of the use of representation and matching contribution proposed to support the recognition of 3D face scans in the presence of the missing parts. For this experiment, we used the data set FRGC v1.0 includes 943 3D face scanning of 275 people presenting a neutral facial expression. Facial scans are given as 480x 640 matrix size of 3D points along a bit mask showing the available points of the scan (i.e., prominent points corresponding typically to the shoulders and head). Since as dissimilar topics distances from the sensor during the acquisition, the actual number of effective's points in a scanning can differ. Persons were acquired with front view of the shoulder, with very small variations in pose. Some analyzes include occlusions due to facial hair. More details on FRGC data set can be instituted in [14].

Depth images are obtained with the 3D face models according to the procedural changes and reported in section 2 pretreatment. [19] According to the proposed contribution, first SIFT key points are extracted range of images from all faces.

This translates into a variable number of key points for the image, depending on the specific characteristics of the surface of the face. To every depth image, just the first 15 key points (selected after ordering all the key points of the coarser the finest scale value) are preserved, and facial profiles are calculated between each pair of these key points.

The validity of the proposed contribution with respect to the missing parts of the face, was tested applying the next experimental settings. The pattern (model) for every topic is selected to form the gallery (i.e., we chose the initial model of each topic as gallery pattern). This showed in a gallery with reference models 275, while all models have been used as probes and compared with those of the gallery. To assess the accuracy of the proposed solution differentiated to parts of the face, every survey face model is divided into two parts (parts of the left and right side with observe to the perfect vertical plane with symmetry since the tip) and the profiles which are derived from a single part of the face differentiated to the gallery scans. Particularly, two corresponding separate experiments were performed first exercising since a probe the left portion of every probe face model, the second by using the right portion of each probe face, the model [19]. The efficiency of recognition has been measured by the rank of recognition rate k and presented cumulative similar characteristics curves (CMC). In special, recognition of rank k experience is successful if the face of the gallery constituting the identical person in the present probe is ranked in first position k of the ranking list. CMC curves evaluated to every value of k, the rate of success rank k experiments.

Fig.2, reports CMC curves for example where just the profiles that come from a region of the face model used for recognition (purple plot refers to the right side with face scanning and green plot refers to the left). To estimate the robustness of the proposed contribution, figure 2 also noted with a CMC blue curves plot for the case where all the profiles are used for recognition. One can observe that no pertinent motion emerges profiles employing the left or right side of the face. The rank 1 recognition rate is adjacent to 80% in the two cases. It is equally attractive to observe that there is just a little decrease in performance compared by the case which the face profiles of the global face [19].

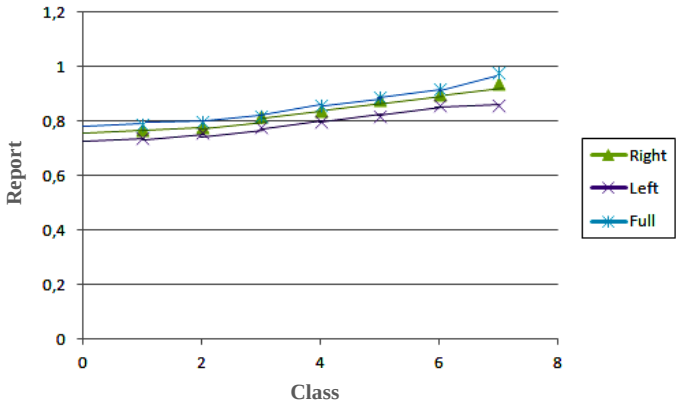

Fig.2 Plots CMC curves obtained using probe models from profiles of key points on the face (blue) left side of the face (purple) and the right side of the face (green).

No large experiences exist on the matching partial 3D face in 3D face recognition literature. To the best of our information, the single performances of work records on 3D face recognition with missing pieces are that of Faltemier and al. [7], until the work in [1] treated only with face occlusions. The approach in [7] can support partial 3D face matching in that it is situated on the correspondence separately different parts of the face to the ICP registration help, and next merging the performances of the individual experience. They reported a rank of recognition rate 1 dataset FRGC v2.0 88% and 89,2%, respectively, for the regions on the left and right side of the face. However, the experimental setting applied in these evaluations completely presumes that the regions are not affected by a corresponding missing part (i.e., parts can fail, but not their parts). Of course, this case is unlikely to occur in real contexts where the missing data can achieve along various measuring a big number of areas. [7] This effect would have a different impact on registration ICP that is not addressed in.

V. Fusion the feature extraction methods with SIFT and LBP

We propose second contribution 3D face recognition based on local properties of the face. The first contribution is improved by the fact that we use SIFT descriptor on LBP image for feature extraction 3D range images. [23] For range images we use the LBP operator, the fusion of the four values of the radius LBP improves performance 2D and 3D information. The LBP operator was at first suggested by Ojala and al. [20] in order to characterize the texture of an image. Calculating the LBP value for each pixel is "threshold" its eight neighbors with a threshold whose value is the gray level of the current pixel. All the neighbors will take a while value 1 if the value is greater than or equal to the current pixel to 0 if the value is less than (Fig.3). The LBP code of the current pixel is then produced by concatenating the 8 values to form a binary code. One thus obtains, as for an image to gray scale, image LBP values containing pixels whose intensity is between 0 and 255.

LBP was subsequently expanded using different sized neighborhoods. In this case, a circle of radius R around the central pixel is considered. The values of sampled points on the P edge of the circle are taken and compared with the value of the central pixel. For values P sample points in the vicinity for any radius R, an interpolation is necessary.

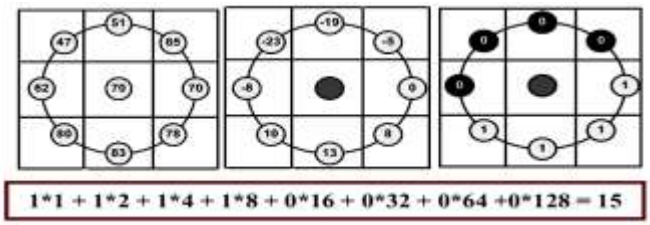

Fig.3 The LBP operator.

We adopt the notation (P, R) for defining the vicinity of points P radius R of a pixel. Fig.4 (a) illustrates three different neighborhoods to R and P values.

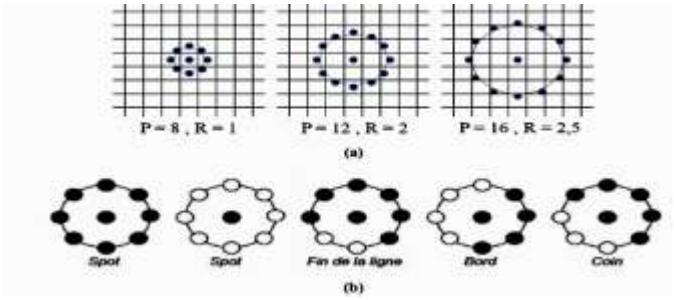

Fig.4 Three different neighborhoods for R and P, (b) detected by specific textures LBP

Where g_c is the gray level of the center pixel, g_p (p = 1 ... P) gray levels of its neighbors, the index LBP of the current pixel is calculated as:

$$LBP_{P,R}(x_c, y_c) = \sum_{p=1}^{p} s(g_p + g_c)\, 2^{p-1} \quad (4)$$

Where

$$s(x) = \begin{cases} 1 & if\ x \geq 0 \\ 0 & if\ x < 0 \end{cases}$$

Where (xc, yc) are the coordinates of the current pixel, P LBP, LBP R is the code for the radius R and the number of neighboring P.

The LBP operator obtained with P = 8 and R = 1 (LBP8, 1) is extremely adjacent to the LBP operator original. The main difference is that the pixels must first be interpolated to get the values of the points on the circle (circular instead of rectangular neighborhood). The important property of the LBP code is that this code is invariant to uniform changes Global

illumination because the LBP of a pixel depends solely on the differences between the level of gray and its neighbors.

Given the depth image and the intensity of the face, we generate a set of LBP multi-scale representation of the face. Some examples are illustrated in Fig.5. In this figure, the number of sampling points varies from 8 points to 24 points and the value of radius ranges from 1 pixel to four pixels.

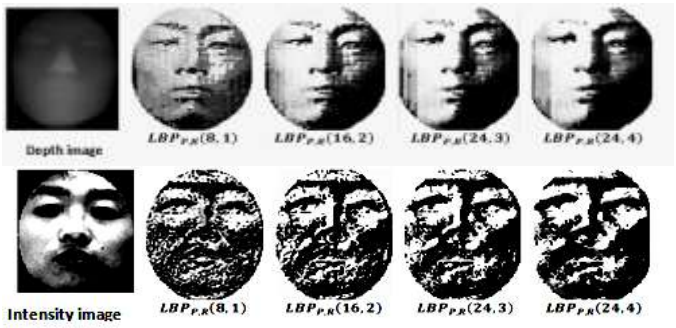

Fig.5 Multi-scale LBP of the depth and intensity image facial.

VI. Experimental Results (2)

We applied the operator SIFT on $LBP_{P,R}$ images separately. Because $LBP_{P,R}$ puts demonstrated smooth local characteristics of the depth image and intensity of the face. One can better detect a number of key points by using SIFT on $LBP_{P,R}$ image, that using of SIFT in the original images. We conducted a statistical work based on data FRGC v1.0.

The average number of extracted key points of each LBP image P, R, is equal to 52 for a depth of 162 images of intensity images. In contrast, the average number of key points extracted from each face image depth of origin is limited to 14. In the intensity, the number of key points is limited to 63.

Fig.6 shows the key points extracted on the image of the original face and its four images $LBP_{P,R}$ associates. To calculate the similarity between the learning face and test the key points of the descriptor SIFT were matched using the Euclidean distance (see Fig.7).

Although the Euclidean distance is optimal in theory, the diverse experiences found that Euclidean distance is surpassed by other distances. One is the cosine [21] which is defined by:

$$S(A,B) = \frac{A^T B}{||A||||B||} \qquad (5)$$

This function simply computes the cosine with the angle among the two feature vectors A and B. A high value of normalized correlation corresponds to a good similarity between the two vectors.

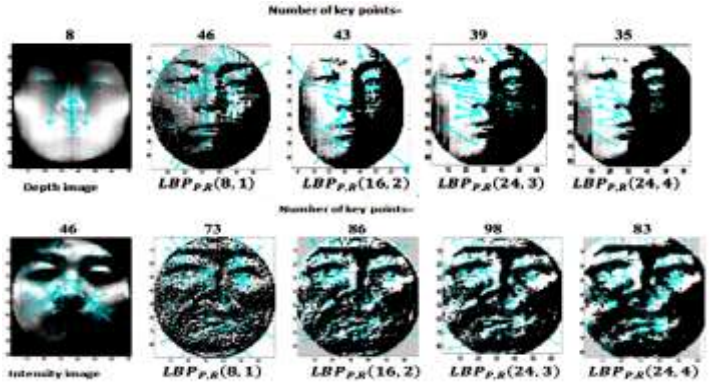

Fig.6 Key points detected with the SIFT descriptor of the depth image and intensity original and four associated images.

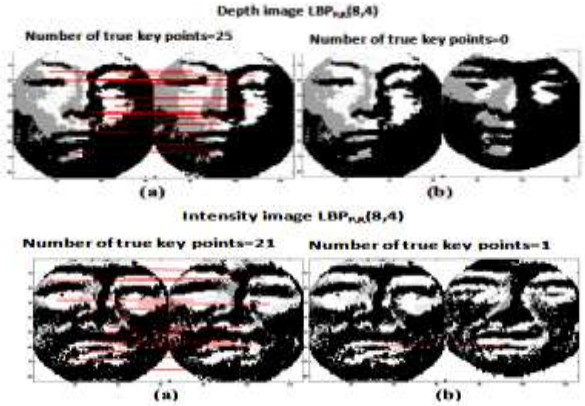

Fig.7 SIFT correspondence between learning and testing faces belonging to (a) the same identity and (b) different identities.

The last step is to verify or reject user requests using a SVM classifier. The table above shows the error rate in all evaluations and testing by this method feature extraction. The number of neighboring points (P) varies from 8 to 24 points and the radius value (R) varies from one to four pixels. LBP method for 3D information provides more performance than the 2D information for four values of the radius (R).

The Table 1 shows the error rate in the total evaluation and test mining by LBP + SIFT features. The number of neighboring points (P) varies from 8 to 24 points and the value the radius (R) varies from one to four pixels. The table shows that the fusion of four LBP (R = 1, 2, 3, 4 and P = 8, 16, 24) plus SIFT works best with a TEE = 4.67% and TV= 94. 98%.

TABLE. 1 SHOWS THE ERROR RATE IN THE TOTAL EVALUATION AND TEST MINING BY LBP + SIFT FEATURES

(P, R)	Intensity Image(2D)		Depth Image(3D)	
	eval	test	eval	test
	TEE	TV	TEE	TV
1-(8, 1)	8.97	81.67	6.73	88.44
2-(16, 2)	6.09	87.47	6.30	89.89
3-(24, 3)	4.18	91.66	7.25	88.7
4-(24, 4)	3.7	89.49	6.34	90.51
1+2+3+4	2.91	92.94	2.67	94.98

VII. CONCLUSION DISCUSSION AND FUTURE WORK

In this work, we proposed a novel contribution to 3D face recognition is capable of recognizing a 3D face model probe also in cases that only a part of the probe model is vacant. The first contribution uses the detection of key points and identification/characterization the key points with SIFT description model on the representation of the range of a face image. Detected key points for identification network profiles, each variation profile representative of the surface with line segments attaching pairs of key points. Our contribution makes no assumption about matching specific markers detected key points on the face. [19] Consequently, it may support comparison network profiles extracted from a probe model versus extraction the network profiles from a model of the same gallery if the model of the probe is only part of the face by employing the SVM algorithm.

First results conducted on the dataset FRGC v1.0 show the viability of the contribution. Comparison with the only alternative approach proposed in the literature by Faltemier and al. [7] suggests that firstly the suggested solution is fewer sensitive than [7] of missing parts, but on the other hand, it needs to be improved to make comparable (if not better) precision values of recognition, the proposed solution get rate 80% for a rank k = 1 with classification data of each face part. However, the approach of S. Berretti, A. Del Bimbo, P.Pala[19] get rate 70% for a rank k = 1 without classification data of each face part. For the latter, the plots reported in figure 2 evidence that the curves for the case where only the profiles that come from a part of the face model used for recognition. This constitutes a probable loss of precision which it highlights the presence of key points and / or profiles that are much equal, while to be extracted from models of different subjects. Using four LBP + SIFT improves our result with TV = 94.98%. Future work will investigate the use of a model to estimate the mutual information between the issues and key points / profiles so as to identify the key points / profiles that can be reliably associated with models a single subject, and we are looking to use FRGC V2.0 database. Multimodality will be approached from the angle appearance, more as a form in first manner; and various scores on various parts of the face (eg, eyes, mouth) combining together in another manner.

REFERENCES

[1] N. Aly uz, B. G okberk, and L. Akarun. 3d face recognition system for expression and occlusion invariance. In IEEE 2nd International Conferance on Biometrics, September 2008.

[2] S. Berretti, A. Del Bimbo, and P. Pala. 3d face recognition using iso-geodesic stripes. IEEE Transactions on Pattern Analysis and MachineIntelligence, 2010.

[3] S. Berretti, A. Del Bimbo, P. Pala, B. Ben Amor, and M. Daoudi. Selected sift features for 3d facial expression recognition. Turkey, August 2010.

[4] K. W. Bowyer, K. I. Chang, and P. J. Flynn. A survey of approaches and challenges in 3d and multi-modal 3d+2d face recognition. January 2006.

[5] K. I. Chang, K. W. Bowyer, and P. J. Flynn. Multiple nose region matching for 3d face recognition under varying facial expression. IEEE, 28(6), pp. 1695-1700, October 2006.

[6] A. Colombo, C. Cusano, and R. Schettini. Gappy pca classication for occlusion tolerant 3d face detection. Journal of Mathematical Imaging and Vision, 35, pp. 193-207, 2009.

[7] T. C. Faltemier, K. W. Bowyer, and P. J. Flynn. A region ensemble for 3d face recognition. IEEE Transactions on Information Forensics and Security,3(1), pp. 62-73, March 2008.

[8] I. A. Kakadiaris, G. Passalis, G. Toderici, N. Murtuza, Y. Lu, N. Karampatziakis, and T. Theoharis. Three-dimensional face recognition in the presence of facial expressions: April 2007.

[9] D. Lowe. Distinctive image features from scale-invariant key points. International Journal of Computer Vision, 60(2):91{110, Nov. 2004.

[10] M. Mayo and E. Zhang. 3d face recognition using multiview key point matching. In IEEE International Conference on Advanced Video and Signal Based Surveillance, pages 290{295,Italy, September 2009.

[11] A. S. Mian, M. Bennamoun, and R. Owens. An ecient multimodal 2d-3d hybrid approach to automatic face recognition. IEEE Transactions on Pattern Analysis and Machine Intelligence, 29(11), pp. 1927-1943, November 2007.

[12] A. S. Mian, M. Bennamoun, and R. Owens. Keypoint detection and local feature matching for textured 3d face recognition. International Journal of ComputerVision, 79(1), pp. 1-12, August 2008.

[13] R. Ohbuchi and T. Furuya. Scale-weighted dense bag of visual features for 3d model retrieval from a partial view 3d model. In Proc. Workshop on Search in 3D and Video, Kyoto, Japan, Sept. 2009.

[14] P. J. Phillips, P. J. Flynn, T. Scruggs, K. W. Bowyer, J. Chang, K. Ho man, J. Marques, J. Min, and W. Worek. Overview of the face recognition grand challenge. In IEEE Workshop on Face Recognition Grand Challenge Experiments, pp. 947-954, San Diego, CA, June 2005.

[15] A. Savran, N. Aly□ uz, H. Dibeklioglu, O. Celiktutan,B. G□ o, B. Sankur, and L. Akarun. Bosphorus database for 3d face analysis. In Proc. First COST 2101 Workshop on Biometrics and Identity Management, May 2008.

[16] W. Zheng, H. Tang, Z. Lin, and T. S. Huang. A novel approach to expression recognition from non-frontal face images. In Proc. IEEE Int. Conf. on Computer Vision, pp. 1901-1908, Kyoto, Japan, Sept. 2009.

[17] Atia Amina. Face recognition in Computer biometric authentication, for academic Master inComputer science , June 2011.

[18] A. Del Bimbo, P. Pala. Recognition of 3D Faces with Missing Parts based on Profile Networks, In Proceedings of the ACM workshop on 3D object retrieval(3DOR '10). ACM, USA, pp. 81-86, 2010.

[19] S. Berretti, A. Del Bimbo, P. Pala. Facial curves between keypoints for recognition of 3D faces with missing parts. IEEE Computer Society Conference on Computer Vision and Pattern Recognition Workshops (CVPRW), 2011, pp.46-51, 20-25 June 2011.

[20] D. Harwood, T. Ojala, M. Pietikäinen, S. Kelman, and S. Davis. Texture Classification by Center-Symmetric Auto-correlation, Using Kullback Discrimination of Distributions. Computer Vision Laboratory, University of Maryland, College Park, Maryland, 1993.

[21] W. Hwang, H. Wang, H. Kim, S. C. Kee, and J. Kim. Face Recognition System Using Multiple Face Model of Hybrid Fourier. IEEE Transactions on Image Processing, vol. 20, no. 4, pp. 1152- 1165, 2011.

[22] H. Tang, B. Yin, Y. Sun , Y. Hu. 3D face recognition using local binary patterns, Signal Processing, vol. 93, pp. 2190-2198,2013.

[23] Abdelmalik OUAMANE. Biometric recognition Multimodal fusion of 2D and 3D Face, for Doctor of Science in Electronics, June 2015.